Heliyon 10 (2024) e27603

Contents lists available at ScienceDirect

Heliyon

journal homepage: www.cell.com/heliyon

Research article

Mechanisms of action of Shizhenqing granules for eczema treatment: Network pharmacology analysis and experimental validation

Hairong Zhang [b], Zhenbo Li [c], Yike Sun [a], Wenna Li [d], Xiao Sun [a], Yapeng Zhang [a], Leilei Liu [a,**], Shuran Ma [a,*]

[a] School of Traditional Chinese Medicine, Beijing University of Chinese Medicine, Beijing, 102488, China
[b] Department of Integrated Chinese and Western Medicine, Yantai Yuhuangding Hospital, Yantai, 264000, Shandong, China
[c] Oregon College of Oriental Medicine, Portland, OR, 97209, USA
[d] Department of Acupuncture and Minimally Invasive Oncology, Beijing University of Chinese Medicine Third Affiliated Hospital, Beijing, 100029, China

ARTICLE INFO

Keywords:
Shizhenqing granules
Eczema
Network pharmacology
Molecular docking
Inflammatory response

ABSTRACT

Background: Jiuwan decoction has been used to treat chronic eczema since the Qing Dynasty. According to clinical experience, Shizhenqing granules (SZQG), derived from the Jiuwan decoction, exert beneficial clinical effects on acute eczema and reduce recurrence. Therefore, we elucidated the underlying mechanisms of SZQG through network pharmacology, molecular docking, and experimental validation.

Methods: The main chemical components of SZQG were identified by ultra-high-performance liquid chromatography-tandem mass spectrometry (UHPLC-MS/MS). And the targets of SZQG against eczema were screened out through online databases. Then, the regulatory network map of the "herbal compound–potential target" and the target protein-protein interaction (PPI) network was constructed. The Gene Ontology (GO) analysis and the Kyoto Encyclopedia of Genes and Genomes (KEGG) pathway enrichment analyses were conducted using by R language. Additionally, the interaction between the active compounds and the targets was verified by molecular docking technology. Finally, an experiment *in vivo* was used to verify the effect and mechanism of SZQG on eczema.

Results: Using UHPLC-MS/MS, 158 main chemical compounds of SZQG were identified, and 72 compounds were selected according to the criteria for further analysis. All 237 potential targets of SZQG in eczema were explored using multiple online databases. The network with 14 core targets was screened out, including STAT3, RELA, TNF, JUN, MAPK3, IL-6, PIK3CA, STAT1, MAPK14, MAPK1, IL-4, NFKBIA, IL1B, and MYC. KEGG analyses indicated that the therapeutic effects of SZQG on eczema were predominantly associated with cytokine-cytokine receptor interaction, TNF, MAPK, NF-κB, toll-like receptor, T cell receptor, and Th1 and Th2 cell differentiation signaling pathways. Furthermore, the good affinity between the core compounds and core targets was verified by molecular docking technology, particularly for RELA and MAPK. Animal experiments revealed that SZQG downregulated MAPK14, RELA, T-bet, and GATA3 mRNA expression,

* Corresponding author.
** Corresponding author.
E-mail addresses: lightloving@126.com (L. Liu), msr13810398297@163.com (S. Ma).

https://doi.org/10.1016/j.heliyon.2024.e27603
Received 4 May 2023; Received in revised form 3 March 2024; Accepted 4 March 2024
Available online 8 March 2024
2405-8440/© 2024 The Authors. Published by Elsevier Ltd. This is an open access article under the CC BY-NC license (http://creativecommons.org/licenses/by-nc/4.0/).

reduced immunoglobulin E (IgE) and interleukin-4 (IL-4) serum concentrations, and improved eczema-like lesions in model rats.

Conclusion: This study identified potential targets and signaling pathways of SZQG in the treatment of eczema, whereby RELA and MAPK14 may constitute the main therapeutic targets of SZQG in cytokine regulation and reduction of inflammatory responses.

1. Introduction

Eczema is a common clinical allergic skin disease; patients with eczema are prone to have chronic illness and recurrent attacks. In the acute phase, eczema is characterized by erythema, continuous pruritus, inflammatory exudation, scaling, and crusting [1]. Epidemiological surveys indicate that the incidence of eczema has been increasing in recent years, particularly in developed countries, in which the incidence is up to 20% in children and 10% in adults [2]. Chronic pruritus leads to anxiety, irritability, and depression, which can severely impact the quality of life and mental health of patients [3]. The underlying pathogenesis involves complex interactions between genetic factors, environmental factors, microbial colonization, skin barrier disorder, and abnormal immune reactions [4,5]. Modern studies have shown that the imbalance of T cell subsets (Th1/Th2) is an important driver of eczema. A dominant Th2 response leads to B cell activation and excessive immunoglobulin E (IgE) secretion, which are key to the pathological features of eczema [6]. Anti-eczema drugs include oral antihistamines, immunomodulators, local glucocorticoids, antimicrobial agents, and emollients [2]. Although these drugs have beneficial acute effects, numerous adverse side effects can occur after long-term use, resulting in drug resistance and high recurrence rates after drug withdrawal [7]. Therefore, alternative treatments to Western drugs must be developed to reduce dissatisfaction with treatment, improve the quality of life, and avoid disease recurrence.

Traditional Chinese Medicine (TCM), as a branch of complementary medicine, is characterized by a systematic, holistic philosophy

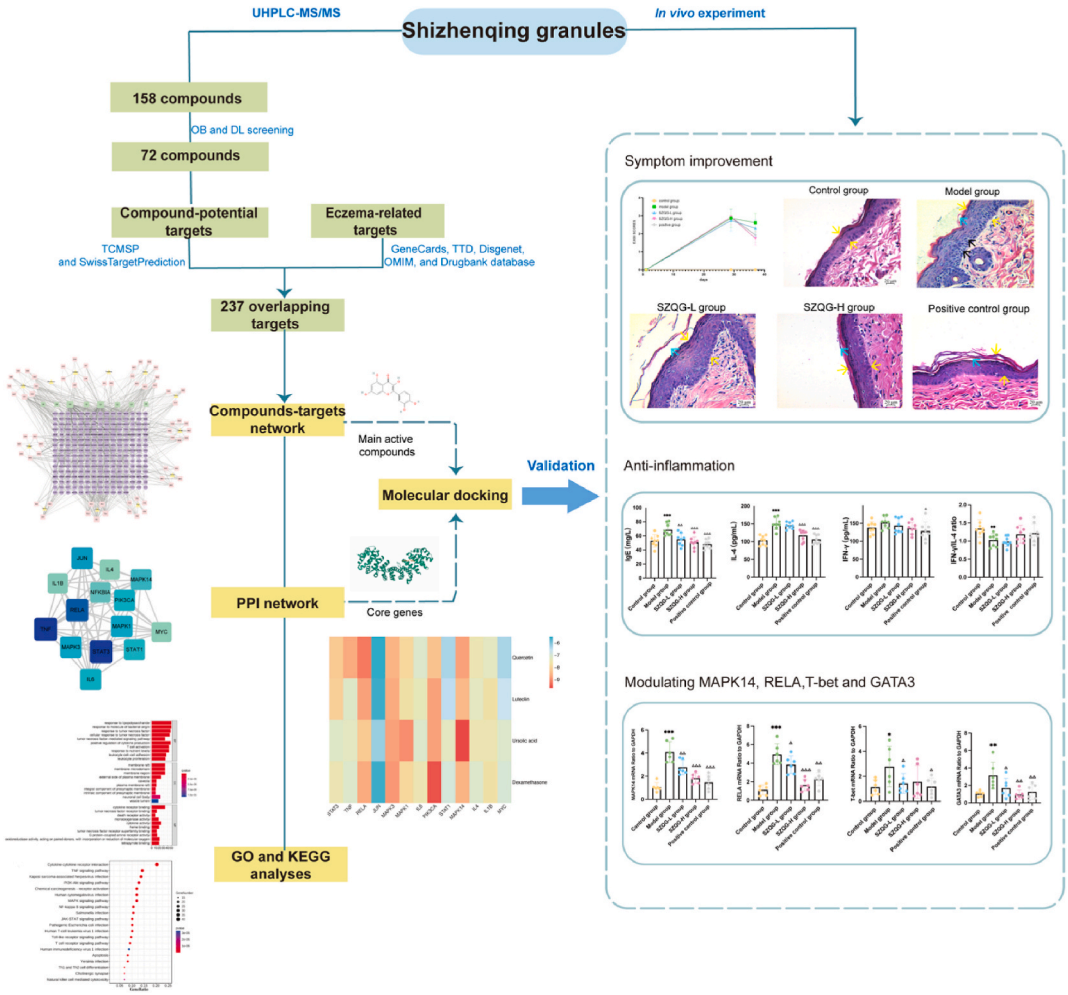

Fig. 1. Workflow in this study.

and traditional theories on the etiology, pathogenesis, and treatment of eczema. Skin diseases are often treated by addressing internal causes in TCM. For example, stubborn skin diseases that cannot be cured for a long time are often treated by promoting qi and blood circulation, clearing heat, and drying dampness, to treat the root cause and symptoms. Extensive preclinical and clinical evidence suggests that both internal and external TCM treatments exert beneficial effects as a treatment for eczema [8]. Shizhenqing granules (SZQG), derived from the Jiuwan decoction of Chen Shiduo during the Qing Dynasty (1636–1912 AD), consist of 12 herbal drugs: *Astragalus membranaceus* (Fisch.) Bge. var. *mongholicus* (Bge.) Hsiao [*Leguminosae; Astragali radix*; Huangqi in Chinese, HQ], *Atractylodes Macrocephala* Koidz. [*Compositae*; *Atractylodis Macrocephalae rhizome*; Baizhu in Chinese, BZ], *Bupleurum chinense* DC. [*Apiaceae*; Bupleur*i radix*; Chaihu in Chinese, CH], *Angelica sinensis* (Oliv.) Diels [*Apiaceae*; *Angelicae sinensis radix*; Danggui in Chinese, DG], Poria cocos (Schw.) Wolf [*Polyporaceae*; *Poria*; Fuling in Chinese, FL], *Pinellia ternata* (Thunb). Breit. [*Araceae*; *Pinelliae rhizoma*; Banxia in Chinese, BX], *Saposhnikovia divaricata* (Turcz.) Schischk. [*Apiaceae*; *Saposhnikoviae radix*; Fangfeng in Chinese, FF], *Forsythia suspense* (Thunb.) Vahl [*Oleaceae*; *Forsythiae fructus*; Lianqiao in Chinese, LQ], Cornus officinalis Sieb. & Zucc. [*Cornaceae*; *Corni fructus*; Shanzhuyu in Chinese, SZY], *Aconitum carmichaeli* Debx. [*Ranunculaceae*; *Aconiti lateralis radix praeparata*; Fuzi in Chinese, FZ], and *Sophora flavescens* Ait. [*Leguminosae*; *Sophorae flavescentis radix*; Kushen in Chinese, KS], and *Glycyrrhiza uralensis* Fisch. [*Leguminosae*; *Glycyrrhizae radix et rhizome*; Gancao in Chinese, GC]. Jiuwan decoction is mainly used for treating intractable skin sores. A previous study has shown that Jiuwan decoction exerts a satisfactory therapeutic effect on model rats with eczema, as it is able to improve serum cortisol, reduce the secretion of cytokines, and regulate immune function [9]. Clinical application has demonstrated that SZQG derived from Jiuwan decoction are effective. We speculated that their underlying mechanism of action may be related to regulating the Th1/Th2 balance and concentration of cytokines. SZQG is a pure herbal prescription with no apparent side effects, which is a therapeutic advantage. Therefore, it is worth further development and utilization.

Network pharmacology is an effective approach for studying the mechanisms of action of TCM prescriptions and can be used to predict the target proteins. Molecular docking is a computational method used to simulate and calculate the binding affinity and binding mode of small molecule compounds with target proteins, in order to find the lowest energy conformation. It plays a crucial role in the development of new drugs by aiding in the identification of potential drug candidates [10,11]. Ultra-high-performance liquid chromatography-tandem mass spectrometry (UHPLC-MS/MS) is an analytical method for the precise identification of drug components. In this study, we first determined the specific compound composition of SZQG. Then, network pharmacology and molecular docking technology were used to predict the therapeutic targets of the main compounds and regulatory networks of SZQG. Finally, these predictions were confirmed in a rat model of eczema. The overall study design is illustrated in Fig. 1.

2. Materials and methods

2.1. Compound analysis of SZQG using UHPLC-MS/MS

2.1.1. Chemicals and reagents

SZQG, composed of 15 g kS, 10 g DG, 10 g HQ, 10 g BZ, 10 g CH, 10 g FL, 10 g FF, 10 g LQ, 6 g GC, 6 g BX, 6 g SZY, and 5 g FZ, were processed into 16 g water-soluble granules by Beijing Tcmages Pharmaceutical Co., Ltd (Beijing, China), according to the TCM decoction method. Detailed information and the production process are shown in Supplementary Table S1.

Eight pure compounds were selected as standard substances (purity ≥98%). Chlorogenic acid (MUST-17030620) was purchased from Chengdu Munster Biotechnology Co., Ltd (Chengdu, China). Baicalin (P20A9F59353) was purchased from Shanghai Yuanye Biotechnology Co., Ltd (Shanghai, China). Liquiritin (11610–201908), adenine (110886–201102), adenosine (110879–201703), benzoylmesaconine (111795201604), benzoylhypaconine (111796–201705), and hypoaconitine (110798–201609) were purchased from National Institute for Food and Drug Control (Beijing, China). Acetonitrile, formic acid, and methanol (chromatography-grade) were purchased from Thermo Fisher Scientific (Fair Lawn, NJ, USA). Distilled water was purchased from Watsons Distilled Water Co., Ltd (Shenzhen, China).

2.1.2. Sample solution preparation

Three grams of SZQG was accurately weighed and extracted in 25 mL of 70% methanol by sonication for 30 min. After extraction, a certain amount of 70% methanol was added to compensate for the weight loss. Then, the solution was placed in a centrifuge tube and centrifuged at 4000×*g* for 10 min, and the supernatant was filtered through a 0.22 μm membrane. Finally, the solution was steamed at 40 °C to recover the solvent and redissolved in 70% methanol (12.5 mL). The solution was stored at 4 °C until further use.

Standard substances (1 mg) were accurately weighed to be placed in a 10 mL volumetric flask and diluted to the volumetric mark using 70% methanol. Then, 1 mL of this mixed standard solution was taken and diluted 10 times using 70% methanol and shaken well.

2.1.3. UHPLC-MS/MS conditions

Liquid chromatographic separation and mass spectrometric detection were performed using a U3000 system coupled with a Q-Exactive-Obitrap MS (Thermo Scientific, Austin, TX, USA). Gradient elution was performed using Waters Acquity UHPLC BEH-C_{18} (1.7 μm, 2.1 × 100 mm) at a flow rate of 0.2 m/min under a column temperature of 30 °C. The injection volume was 5 μL. The mobile phase was composed of water containing 0.1% formic acid (A) and acetonitrile (B) with the following gradient elution procedure: 0–9 min, 96%–87% A; 9–30 min, 87%–75% A; 30–45 min, 75%–40% A; 45–55 min, 40%–0% A; 55–56 min, 0% A; 56–58 min, 0%–96% A; 58–63 min, 96% A. A mass spectrometer equipped with heated electrospray ionization (HESI) source was operated in both positive and negative ion modes with the following parameters: scanning range, 100–1400 Da; ion spray temperature, 350 °C; ionization source voltage, 4 kV; capillary voltage, 35 V; and tube lens voltage, 110 V. Nitrogen was used as the auxiliary gas and sheath gas at pressures

of 20 and 40 psi, respectively.

2.1.4. Data analysis

The collected data were analyzed using the Xcalibur 4.2 workstation (Thermo Scientific) with a standard of quality deviation of $\delta \leq 10 \times 10^{-6}$. The chemical composition was confirmed in the PubChem (https://pubchem.ncbi.nlm.nih.gov/) and related references based on the chromatographic behavior of samples, excimer ion peaks of mass spectrometry, ion fragments, and other information, combined with reference materials and relevant characteristic fragments.

2.2. Network pharmacology analysis

2.2.1. Identification of potential targets of SZQG in eczema

According to the criteria of absorption, distribution, metabolism, and excretion in the Traditional Chinese Medicine Systems Pharmacology Database and Analysis Platform (TCMSP) [12] (https://old.tcmsp-e.com/tcmsp.php), the compounds verified by UHPLC-MS/MS were ulteriorly filtered based on measure of oral availability (OB) $\geq$ 30% and drug-likeness (DL) $\geq$ 0.18 [13]. All candidate target genes of the main compounds were obtained from TCMSP and SwissTargetPrediction [14] (http://www.swisstargetprediction.ch/). The known targets of the compounds were identified according to the published literature. After the removal of duplicates, potential targets were standardized using the UniProt protein database [15] (https://www.uniprot.org).

Keywords such as "eczema" or "atopic dermatitis" were used to search for targets related to the pathogenesis of eczema from five databases: GeneCards [16] (https://www.genecards.org), TTD [17] (http://db.idrblab.net/ttd/), Disgenet database [18] (https://www.disgenet.org), OMIM [19] (https://omim.org/), and Drugbank database [20] (https://www.drugbank.ca/). Duplicate values were removed.

2.2.2. Construction of the "herbal compound–potential target" regulatory network of SZQG

Using the Venny 2.1 tool (https://bioinfogp.cnb.csic.es/tools/venny/), the overlapping targets between the identified compounds and disease were obtained to construct a Venn diagram. A regulatory network map of the overlapping targets and compounds was constructed using Cytoscape software (V3.8.0, National Institute of General Medical Sciences, Bethesda, MD, USA).

2.2.3. Construction of the protein-protein interaction (PPI) network

The PPI network of candidate genes was constructed using the STRING database [21] (https://string-db.org/), with filtration of the highest confidence of 0.9. The results were imported into Cytoscape, and the CytoNCA plug-in was used for network topology analysis to identify core target genes.

2.2.4. Gene Ontology (GO) and Kyoto Encyclopedia of Genes and Genomes (KEGG) pathway enrichment analysis

GO and KEGG were performed using the Biocmanager, Bioconductor, DOSE, and Enrichplot packages of R (V4.1.0 Microsoft Corporation, Redmond, WA, USA), followed by visualization of the results.

2.3. Molecular docking simulation

Molecular docking was used to predict the connection type and binding ability of the core compounds of SZQG (ligand) interacting with target proteins (receptors). The 2D structures of these compounds were downloaded from PubChem (https://pubchem.ncbi.nlm.nih.gov/). Chem3D was used to generate the 3D structure of ligands and minimize the energy. After downloading the 3D images of target protein molecules from the PDB database (http://www1.rcsb.org/), water and solvent were removed from the receptor using PyMOL software (Schrödinger Inc, New York, NY, USA). AutoDock Tools (Scripps Research Institute, La Jolla, CA, USA) was used to convert the formats of the ligand and receptor files and to add hydrogen atoms and electrons to the receptor. Subsequently, the appropriate active pocket of the receptor was set using AutoDockTools. Finally, molecular docking was performed using Vina software (The Center for Computational Structural Biology, La Jolla, CA, USA), and the results were imported into PYMOL software for visual processing.

2.4. Animal experimental validation

2.4.1. Drug preparation

After conversion into water-soluble granules, the dosage of SZQG for a standard human was 0.27 g/kg/day. According to the body surface area conversion, the gavage dose for rats was 1.68 g/kg/day [22]. SZQG were dissolved in hot purified water, prepared in liquid at 168 mg/mL, and then stored at 4 °C. Dexamethasone (DEX, Zhejiang Xianju Pharmaceutical, Taizhou, China) was used as a positive control in this study. DEX was mixed with pure water into 0.0315 mg/mL liquid medicine and stored at 4 °C.

2.4.2. Animal modeling and grouping

In total, 40 male Sprague-Dawley (SD) rats (200 $\pm$ 10 g, 4 weeks old; SPF) were purchased from SPF (Beijing) Biotechnology Co., Ltd. (Beijing, China, No.: SCXK[Jing]2019-0010). The animals were raised in a standard laboratory environment with free access to food and water. All experiments were performed in accordance with the Guidelines for the Care and Use of Laboratory Animals. The Medical and Experimental Animal Ethics Committee of Beijing University of Chinese Medicine approved this experiment (Approval

No.: BUCM-4-2021110806-4069). After 5 days of acclimatization, the animals were divided into five groups randomly: control, model, low-dose SZQG (SZQG-L) (0.56 g/kg/day), high-dose SZQG (SZQG-H) (1.68 g/kg/day), and positive control (DEX treatment) groups, with eight rats in each group. With the exception of the control group, the remaining groups were used to develop eczema models based on previous studies [22,23]. The back fur of rats was removed using depilation cream 1 day before 2,4-dinitrochlorobenzene (DNCB) treatment. The back was then divided into two areas, A and B, and 100 μL of 7% DNCB acetone solution was topically applied to sensitize area A. After 7 days, area B was treated with 200 μL of 5% DNCB once every 5 days, four times in a row. The appearance of desquamation, erythema, and other conditions on the back was observed on day 29, supporting the success of modeling. After modeling, the treatment groups were administered 1 mL/100 g of the corresponding drug liquid, whereas the control and model groups were administered the same dose of purified water. After 7 days of treatment, the rats were fasted for more than 12 h. Subsequently, rats were anesthetized by intraperitoneal administration of 3% pentobarbital sodium (40 mg/kg), and the blood was collected from the abdominal aorta to induce death.

2.4.3. Skin lesion observation

According to the Eczema Area and Severity Index (EASI), symptoms of erythema, edema, excoriation, and dryness were divided into four grades [24]. The relative severity of each symptom in rats was determined using the scoring method as follows: 0 (none), 1 (mild), 2 (moderate), and 3 (severe). The skin lesions of rats in each group were scored and recorded on days 29 and 37 of experimentation.

2.4.4. Histopathological analysis

After the rats were sacrificed, the skin lesions were fixed with 10% formalin to prepare paraffin-embedded skin sections. Skin sections were stained with hematoxylin and eosin (H&E) to observe pathological changes in the skin, according to the standard laboratory protocol [25]: hematoxylin was applied for 5 min, followed by differentiation in 1% HCl ethanol for 5 s, and then eosin was applied for 5 min. The sections were observed with a Leica DMC5400 microscope (GERMAN, Leica) and the thickness of the epidermal tissue in each group was recorded.

2.4.5. Enzyme-linked immunosorbent assay analysis

After being left at room temperature for 2 h, the serum was separated from abdominal aortic blood by centrifugation at 700×*g* for 30 min at 4 °C and stored at −80 °C. Serum immunoglobulin E (IgE), interferon-γ (IFN)-γ, and interleukin-4 (IL-4) levels were measured using enzyme-linked immunosorbent assay kits (BlueGene Biotech Co., Ltd, Shanghai, China) according to the manufacturer's instructions.

2.4.6. Quantitative real-time polymerase chain reaction (qRT-PCR)

Total RNA was extracted from rat skin tissue using a Hipure universal RNA kit (Guangzhou Magen Biotechnology Co., Ltd, Guangzhou, China). After assessing the purity and concentration of the total RNA, cDNA was obtained by reverse transcription with 2 μg of total RNA using a T100™ Thermal Cycler. qRT-PCR was performed on a C1000Touch™ Thermal Cycler with the following reaction conditions: stage 1, 95 °C for 30 s; stage 2, 40 cycles of 95 °C for 10 s and 60 °C for 30 s. The relative quantification of target genes was normalized to that of the internal control gene GAPDH in each sample, which was calculated using the $2^{-\triangle\triangle CT}$ method. The designed primer sequences are shown in Table 1.

2.5. Statistical analysis

Data are expressed as the mean ± standard deviation and were analyzed using SPSS 26.0 (IBM Corp., Armonk, NY, USA) and GraphPad Prism 9.0 (version 9.0, GraphPad Software, San Diego, CA, USA). One-way analysis of variance (ANOVA) was used for statistical analysis, followed by multiple comparison tests with the least significant difference (LSD). Differences were considered significant at $p < 0.05$.

Table 1
Primer sequence information.

Gene	Primer sequence	Size (bp)
RELA	F: 5′-GGATGGCTTCTATGAGGCTGAACTC-3′	98
	R: 5′-CTTGCTCCAGGTCTCGCTTCTTC-3′	98
MAPK14	F: 5′-GATAAGAGGATCACAGCAGCCCAAG-3′	149
	R: 5′-TCGTAGGTCAGGCTCTTCCATTCG-3′	149
T-bet	F: 5′-TCTGTCGAACCAGTATCCTGTCTCC-3′	142
	R: 5′-CTTCACGCTCACTGCTCGGAAC-3′	142
GATA3	F: 5′-TCTGGAGGAGGAACGCTAACGG-3′	122
	R: 5′-CTTACGGTTTCGGGTCTGGATGC-3′	122
GAPDH	F: 5′-GACATGCCGCCTGGAGAAAC-3′	92
	R: 5′-AGCCCAGGATGCCCTTTAGT-3′	92

Note: "F" represents "forward; " "R" represents "reverse."

3. Results

3.1. Identification of the chemical compounds in SZQG by UHPLC-MS/MS

Using UHPLC-MS/MS, 158 main peak compounds were obtained in positive and negative ion modes, among which chlorogenic acid, baicalin, liquiritin, adenine, adenosine, benzoylmesaconine, benzoylhypaconine, and hypoaconitine were determined by comparison with the standard substance (Fig. 2A and B, and Supplementary Table S2). With reference to the existing literature and screening according to the values of OB and DL conditions, 72 compounds, including quercetin, luteolin, and ursolic acid, were selected as candidates for further analysis (Supplementary Table S3 and Supplementary Table S4).

3.2. Target proteins for SZQG and eczema

Among the 72 compounds of SZQG, 1382 potential targets were obtained by combining and removing overlapping values. A total of 2737 known targets were identified from the GeneCards database. Targets with a "relevance score" greater than the median score of 2.92 were selected for further analysis. In total, 790 potential eczema targets were identified. Combined with the OMIM, TTD, DrugBank, and DisDeNET databases, related targets were gathered and duplicated. Finally, we identified 1409 eczema-related targets (Supplementary Table S5).

3.3. Compound-disease target network

Using Venny 2.1, we obtained 237 overlapping genes for SZQG and eczema treatment in the Venn diagram (Fig. 3A). Then, the "herbal compound–potential target" was constructed and included 320 nodes and 928 edges (Fig. 3B, Supplementary Tables S6 and 7).

3.4. PPI network analysis

The 237 candidate targets were uploaded to the STRING database to construct a PPI network. According to the highest confidence score >0.9, a network with 172 nodes and 687 edges was obtained (Fig. 4A). Topological analysis was performed using Cytoscape. Core targets were selected according to the median value of "degree," "betweenness," "closeness," "eigenvector," "network," and "local average connectivity." After performing filtration twice, a core network of 14 nodes, including STAT3, RELA, TNF, JUN, MAPK3, IL-6, PIK3CA, STAT1, MAPK14, MAPK1, IL-4, NFKBIA, IL1B, and MYC, was established (Fig. 4B, Supplementary Table S8).

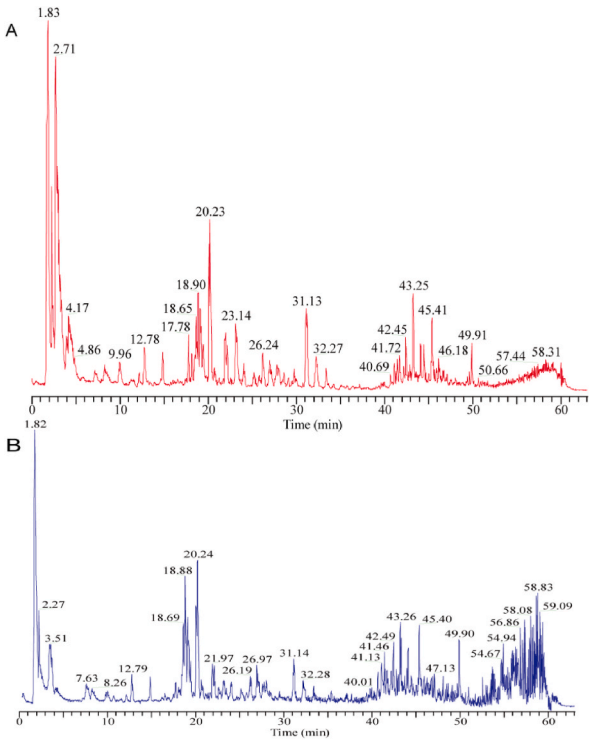

Fig. 2. Total ion chromatogram by UHPLC-MS/MS. (A) Positive ion mode. (B) Negative ion mode.

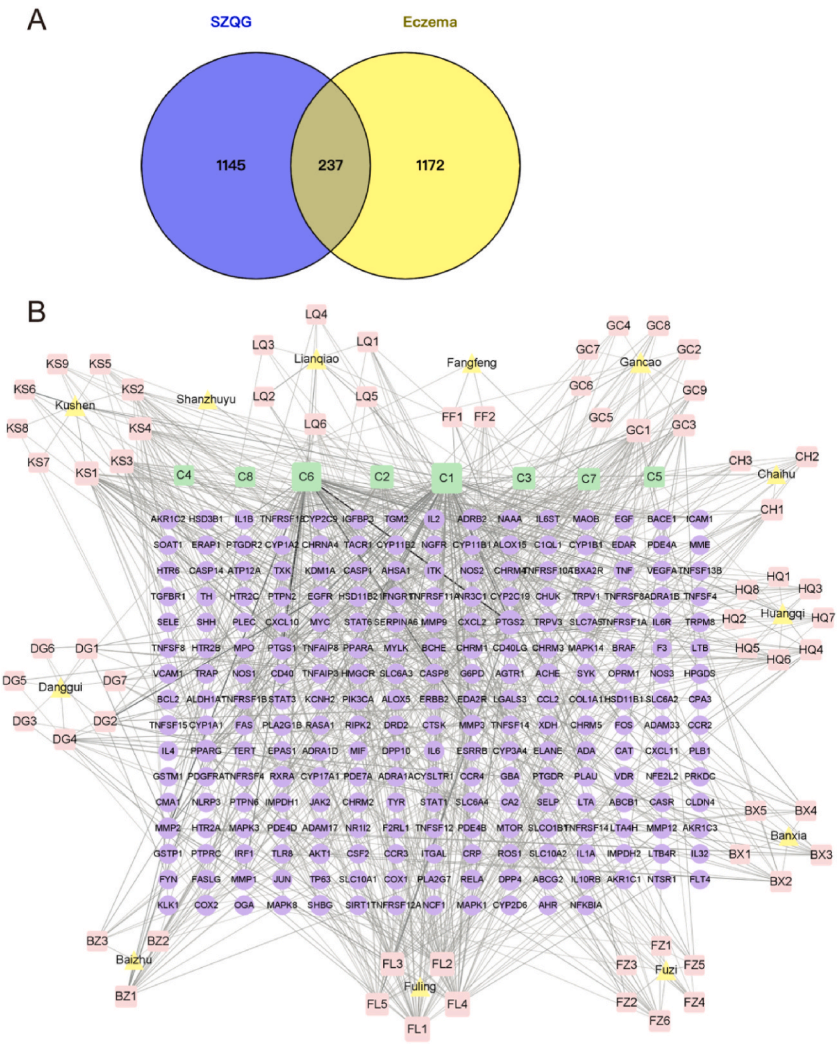

Fig. 3. Overlapping targets and compound-target network construction. (A) Venn diagram of target genes of SZQG and eczema-related genes. (B) Drug compound-potential targets network. The different colors represent different types of nodes. Purple, yellow, pink, and green nodes represent genes, ingredients of SZQG, compounds, and common compounds between drugs, respectively. The lines represent the interactions between nodes, and node size is positively correlated with degree value. (For interpretation of the references to color in this figure legend, the reader is referred to the Web version of this article.)

3.5. GO and KEGG pathway enrichment analysis

Using the BiocManager package of R language software, the names of potential targets of SZQG against eczema were transformed into gene IDs. Subsequently, functional enrichment and KEGG pathway enrichment analyses were conducted using the Bioconductor, dose, and enriched packages. The results were visualized and sequenced according to *p*-values. We identified 2531 items of potential biological process (BP), including response to lipopolysaccharide, response to molecules of bacterial origin, and response to tumor necrosis factor; 47 items of cell components (CC), including membrane raft, membrane microdomain, and membrane region; and 194 items of molecular function (MF), including cytokine receptor binding, tumor necrosis factor receptor binding, and death receptor activity. The top 10 items are presented in Fig. 5A (Supplementary Table S9).

Based on the KEGG pathway enrichment results, 168 KEGG pathways were identified ($p < 0.05$). After excluding broad pathways, the top 20 pathways were selected according to the number of enriched genes (Fig. 5B, Supplementary Table S10). In combination with a literature review [26,27], the key pathways among the top 20 included cytokine-cytokine receptor interaction, tumor necrosis factor (TNF), mitogen-activated protein kinase (MAPK), nuclear factor kappa B (NF-κB), toll-like receptor, T cell receptor, and Th1 and Th2 cell differentiation signaling pathways, which predominantly regulate complex biological immunological processes, such as inflammation and cell differentiation.

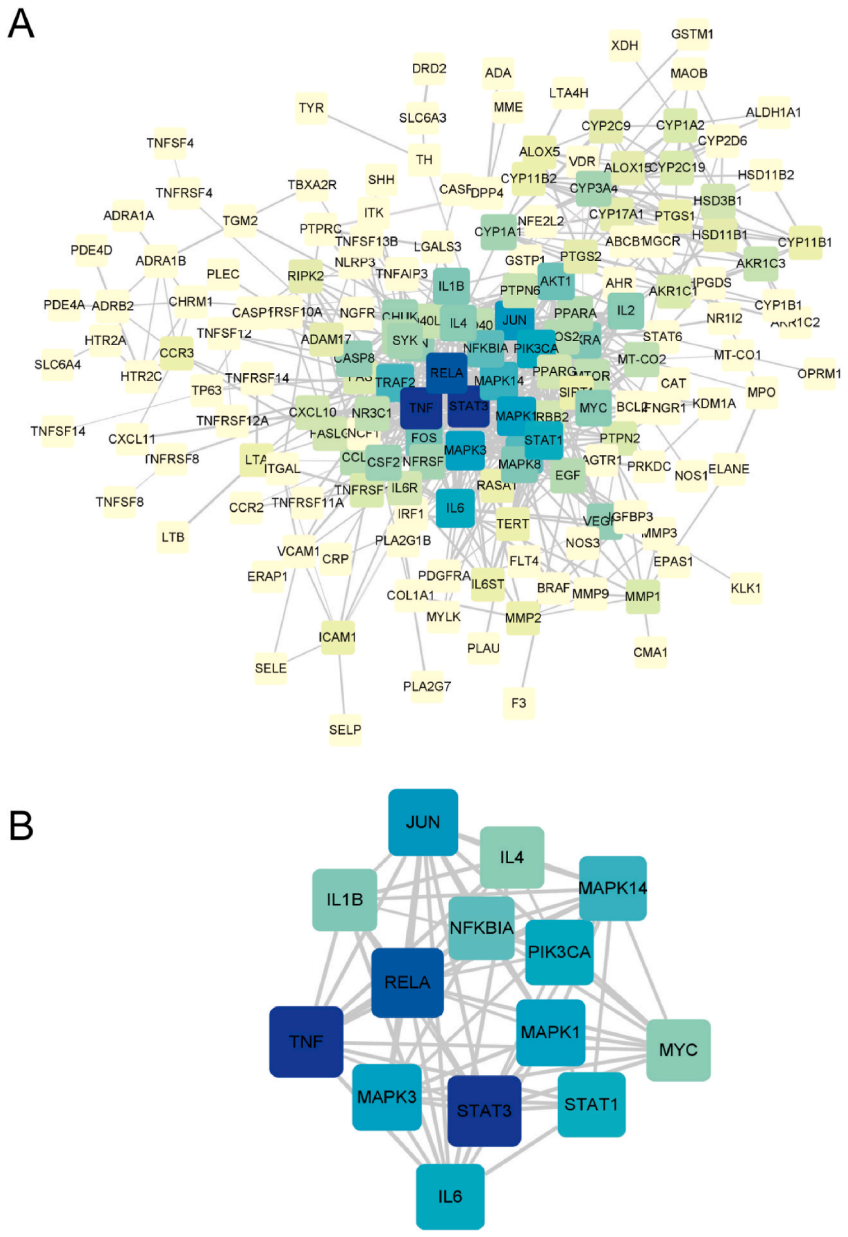

Fig. 4. PPI network construction and screening. (A) PPI network of SZQG against eczema. (B) Core targets. Darker color is correlated with higher degree. (For interpretation of the references to color in this figure legend, the reader is referred to the Web version of this article.)

3.6. Molecular docking results

The top target proteins in the PPI network were selected as receptors for docking with the main compounds (quercetin, luteolin, and ursolic acid) of SZQG. DEX, a drug commonly used for eczema, was used as a reference. The docking results are presented as a heat map in Fig. 6A, except NFKBIA due to the lack of a complete protein structure in the PDB database. The general consensus is that lower binding energy and a higher number of hydrogen bonds are associated with greater stability of a ligand binding to the receptor. Indeed, there is significant binding ability between ligand and receptor when the binding energy is < -5 kcal/mol [28]. The docking results verified that the main compounds of SZQG may bind well to the core target proteins, particularly RELA and MAPK14 (Fig. 6B, Supplementary Tables S11 and S12).

3.7. Effects of SZQG on eczema-like symptoms and EASI scores

Repeated administration of DNCB on rat dorsal skin resulted in clinical eczema-like symptoms, such as erythema, dry

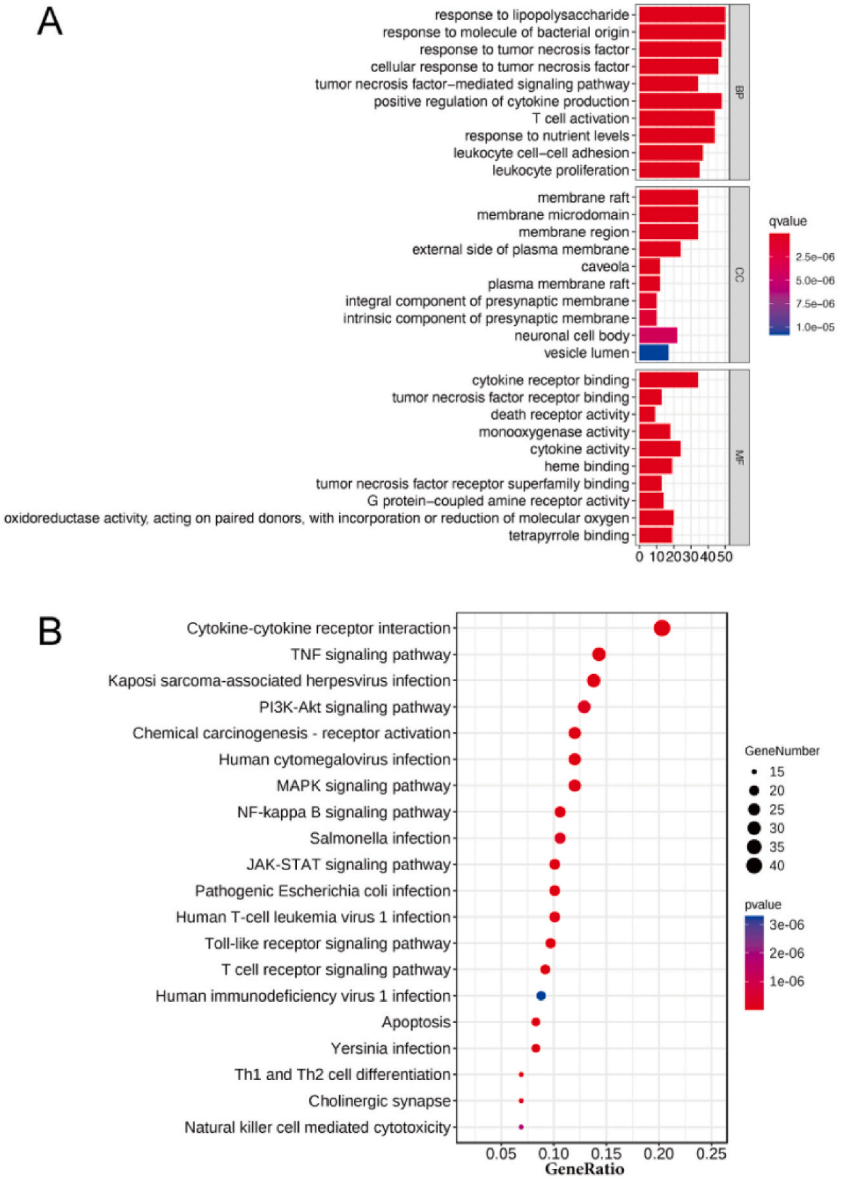

Fig. 5. GO and KEGG analysis. (A) GO functional enrichment of candidate targets. BP, biological process; CC, cellular component; MF, molecular function. The length of the histogram represents the number of genes enriched in the term, and the color indicates the level of significance (red indicates greater significance). (B) Top 20 pathways of KEGG enrichment. The size of the circle indicates the number of enriched genes, and the color indicates the significance (*p*-value). (For interpretation of the references to color in this figure legend, the reader is referred to the Web version of this article.)

desquamation, edema, scabs, and skin roughness (Fig. 7A). Compared with the model group, the SZQG- and DEX-treated rats exhibited a significant alleviation of lesion severity. To quantify lesion severity, EASI scores were calculated on days 1, 29, and 37 (Fig. 7B). The analysis indicated that the DNCB-induced model was successful, and treatment with SZQG and DEX significantly decreased EASI scores. Notably, scores in the SZQG group were lower than those in the positive control group, suggesting that SZQG treatment was more effective for improving symptoms.

3.8. Effects of SZQG on inflammatory infiltration in rat skin lesions

H&E staining showed that the epidermal tissue of the control group was structurally normal and consisted of laminar flattened epithelial cells and keratin. In the model group, the skin of rats had a thickened granular layer and spiny layer, edema of spiny layer cells, and enlarged intercellular gaps. The dermal vessels were dilated and congested with inflammatory infiltration. Treatment with SZQG significantly alleviated skin tissue lesions, including epidermal hyperplasia, dyskeratosis, acanthosis, and tissue edema, as well

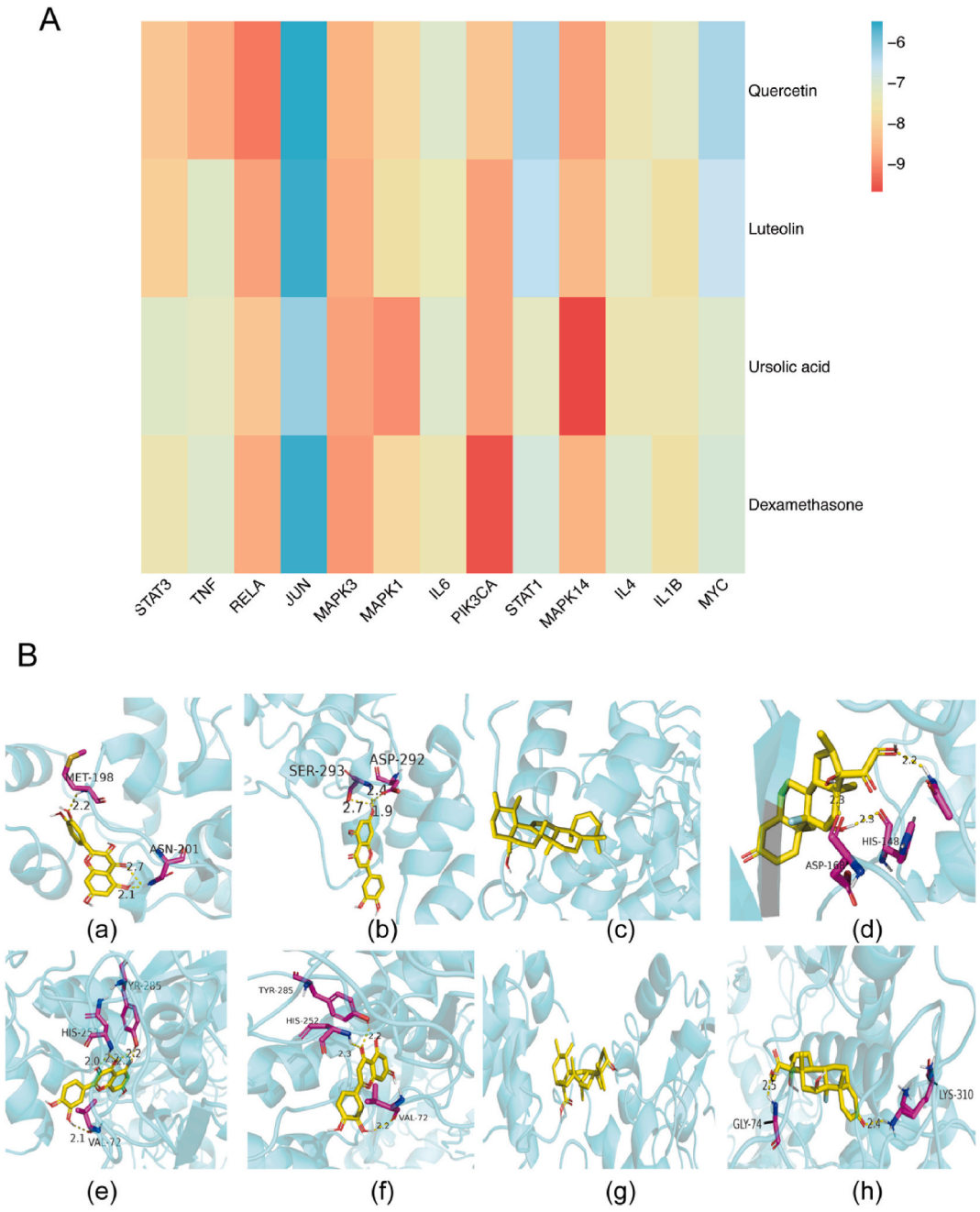

Fig. 6. Molecular docking results. (A) Heat map of molecular docking scores. (B) (a) MAPK14-quercetin, (b) MAPK14-luteolin, (c) MAPK14-ursolic acid, (d) MAPK14-dexamethasone, (e) RELA-quercetin, (f) RELA-luteolin, (g) RELA-ursolic acid, and (h) RELA-dexamethasone.

as inflammatory infiltration. This treatment effect was equivalent to that of DEX treatment (Fig. 8A). The thickness of the epidermal tissue in each group is shown in Fig. 8B.

3.9. Effects of SZQG on serum levels of inflammatory factors

Serum IL-4 and IgE levels were significantly higher in eczema model rats than in control rats ($p < 0.001$) (Fig. 9A and B), whereas the concentration of INF-γ did not change significantly ($p > 0.05$) (Fig. 9C). Comparison between the two treatment groups and model group revealed that SZQG reduced serum levels of inflammatory factors (particularly IL-4 and IgE) in a dose-dependent manner. No significant difference was observed between the SZQG-H and positive control groups. Although SZQG reduced IFN-γ levels, the magnitude of the effect was less than that in the positive control group ($p < 0.05$). Both SZQG and DEX regulated the IFN-γ/IL-4 ratio.

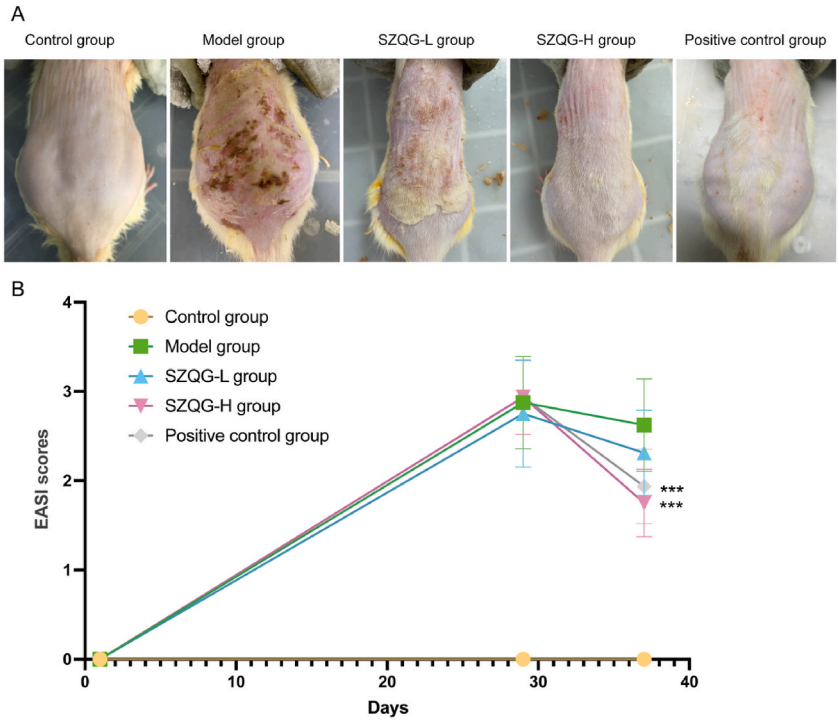

Fig. 7. Effects of SZQG treatment on skin lesions and EASI scores. (A) Representative images of rat dorsal skin in each group. The images were obtained on day 37 of experimentation (before sampling). (B) EASI scores were calculated for skin lesions of rats on days 1, 29, and 37 of experimentation. ***$p < 0.001$ *vs.* pre-treatment scores. Data are expressed as mean ± standard deviation ($n = 8$).

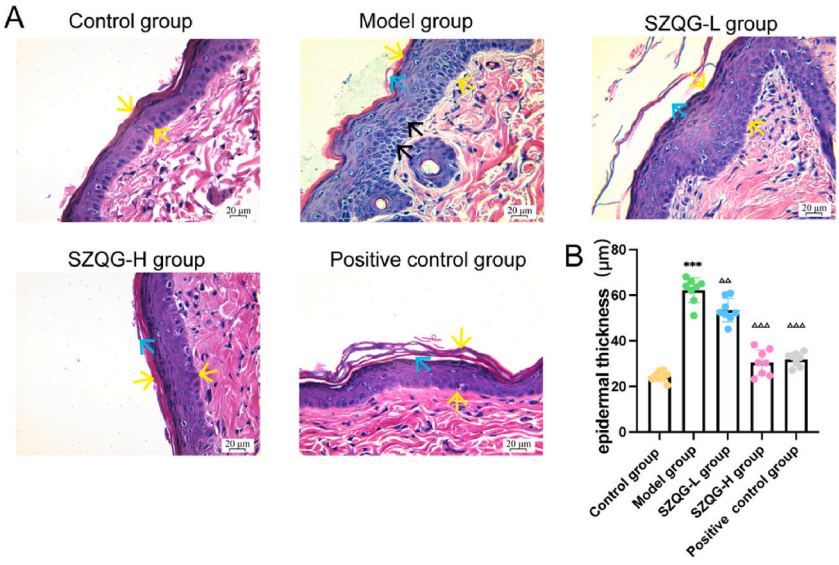

Fig. 8. Effects of SZQG on histopathological sections. (A) H&E staining of the dorsal skin of rats. (B) Epidermal thickness ($n = 8$). Yellow arrows in between represent the epidermal tissue; black arrows represent edema of spinous layer cells; light blue arrows represent parakeratosis. Scale bar = 20 μm. (For interpretation of the references to color in this figure legend, the reader is referred to the Web version of this article.)

However, there was no significant difference compared with the model group ($p > 0.05$) (Fig. 9D).

3.10. Effects of SZQG on RELA, MAPK14, T-bet, and GATA3 mRNA levels in lesions

The skin tissue of the model group had significantly higher RELA and MAPK14 mRNA levels ($p < 0.001$) and T-bet and GATA3

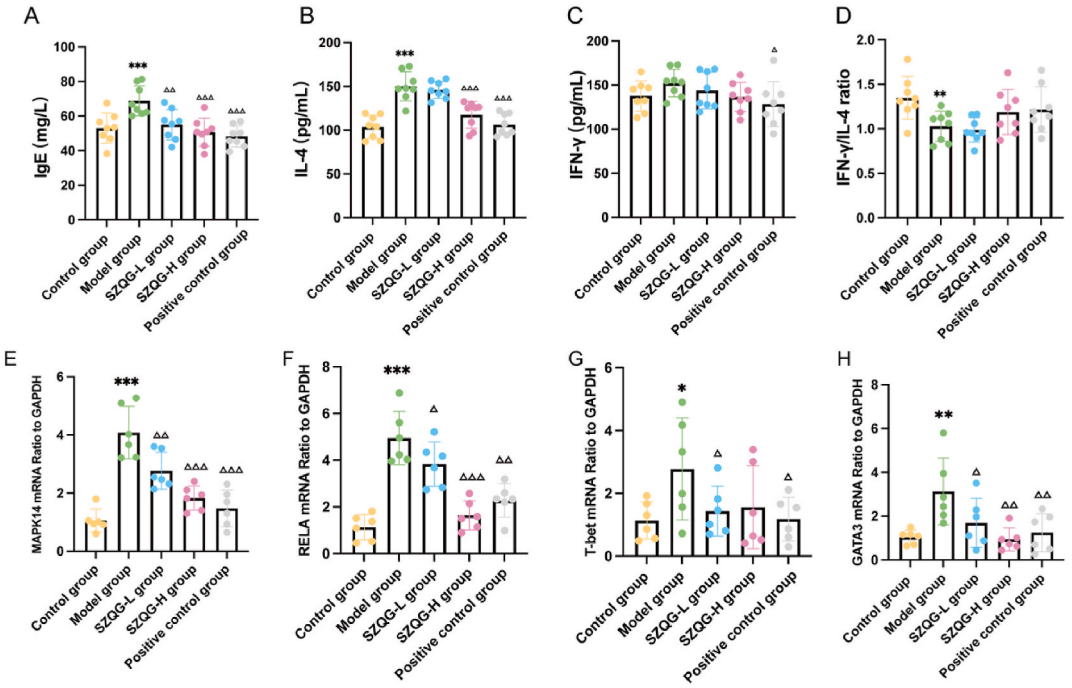

Fig. 9. Effects of SZQG treatment on inflammatory factor, MAPK14, RELA, T-bet, and GATA3 mRNA levels. (A–C) Serum levels of IgE, IL-4, and IFN-γ, respectively ($n = 8$). (D) Serum IFN-γ/IL-4 ratio. (E–G) MAPK14, RELA, T-bet, and GATA3 mRNA levels in skin tissue ($n = 6$). Data are expressed as mean ± standard deviation. $^{**}p < 0.01$, $^{***}p < 0.001$ *vs.* the control group; $^{\triangle}p < 0.05$, $^{\triangle\triangle}p < 0.01$, $^{\triangle\triangle\triangle}p < 0.001$ *vs.* the model group.

expression ($p < 0.05$) than that of the control group. RELA, MAPK14, T-bet, and GATA3 mRNA levels were significantly lower in the treatment groups (SZQG-L, SZQG-H, and positive control groups) than in the model group ($p < 0.05$), implying that SZQG inhibited the expression of MAPK14 and RELA in DNCB-induced inflammation, and intervened the differentiation of Th1 and Th2 by adjusting the ratio of transcription factor T-bet/GATA3. No significant differences in RELA, MAPK14, and GATA3 mRNA levels were observed between the SZQG-H and positive control groups (Fig. 9E–H).

4. Discussion

Eczema is a common inflammatory skin disease with a complex pathogenesis. The general consensus is that eczema is characterized by the induction and activation of inflammatory factors, in which elevated levels of serum IgE and Th2 cytokines constitute typical pathological features [29]. Indeed, inhibiting the expression of inflammatory factors reduces the symptoms of eczema disease [2]. Several medicinal plants have exhibited substantial anti-inflammatory and immunomodulatory effects, such as regulation of immune balance and avoidance of excessive lymphocyte activation [30]. The prescription SZQG used in this study was obtained from the Jiuwan decoction with the addition of KS. Numerous pharmacological experiments have demonstrated that KS has good anti-inflammatory, antibacterial, and anti-allergic effects, alongside a wide application in various skin inflammatory conditions, such as eczema and atopic dermatitis [31]. Using network pharmacology, we constructed a network of core compounds, targets, and signaling pathways, which provided evidence for the multi-target and multi-channel mechanisms of SZQG in the treatment of eczema. Further, we established a rat model of eczema to verify these effects *in vivo*.

In this study, 158 compounds were identified by UHPLC-MS/MS and 72 compounds were screened for follow-up analysis. Our analysis revealed that the core compounds of SZQG in treating eczema were quercetin, luteolin, and ursolic acid. Quercetin, a natural and widely available polyphenolic flavonoid, is present in HQ, CH, LQ, KS, and GS, which are contained in SZQG. It has a good antioxidant effect and can reduce skin oxidative stress damage. Moreover, it can inhibit the production of cytokines such as IFN-γ and IL-4 by downregulating the RAGE/NF-κB signaling pathway, thus playing an anti-inflammatory and anti-allergic role [32]. Quercetin is widely applied in the treatment of atopic dermatitis and actinic dermatitis [33,34]. Ursolic acid, a common component of LQ and SZY, is a natural triterpenoid exhibiting various biological properties, such as anti-inflammatory, immune regulatory, and antioxidant activities. It can effectively inhibit the activation of NF-κB and MAPK in lipopolysaccharide-stimulated macrophages and reduce the synthesis of the inflammatory mediators prostaglandin E2 and nitric oxide [35]. Ursolic acid has been reported to interfere with reactive oxygen species-mediated apoptosis and inflammatory activation induced by ultraviolet B irradiation damage [36]. Luteolin, which belongs to the group of flavonoids, is an important ingredient of LQ and KS. It has been demonstrated to exert anti-oxidation, antimicrobial, and anti-inflammatory effects by inhibiting reactive oxygen species production, reducing inflammatory cytokine and mediator levels, and inhibiting NF-κB, STAT1, and STAT3 expression [37]. In addition, luteolin inhibits mast cell activation and the

release of histamine, leukotriene, and prostaglandin D2 in a concentration-dependent manner, thereby alleviating the symptoms of allergic dermatitis [38]. These aforementioned studies verified that the core compounds of SZQG can regulate inflammation response, which is consistent with the results from the animal experiments conducted in this study.

The core target network of SZQG for the treatment of eczema contains 14 targets: STAT3, RELA, TNF, JUN, MAPK3, IL-6, PIK3CA, STAT1, MAPK14, MAPK1, IL-4, NFKBIA, IL1B, and MYC. These potential targets play key roles in inflammatory pathways. Molecular docking revealed that the binding ability of these targets with core compounds was lower than −5 kcal/mol, showing a good binding ability, among which RELA and MAPK14 exhibited the best binding ability. RELA, also known as P65, is a subunit of the nuclear transcription factor NF-κB complex. RELA generally resides in the cytoplasm and its activity is inhibited by IkappaB-alpha (IκBα). When activated by stress and inflammatory mediators, IκBα is phosphorylated, ubiquitinated, and subsequently degraded. NF-κB enters the nucleus to regulate the expression of genes related to inflammation, immunity, proliferation, and differentiation, and regulates the secretion of various downstream cytokines [39]. It has been demonstrated that the inhibition of p65 phosphorylation in rheumatoid arthritis could decrease IL-4 levels and elevate IFN-γ levels, subsequently adjusting the ratio of Th1 to Th2 cells in the spleen [40]. MAPK14, also known as p38α, is a key component of MAP kinase signal transduction. Stimulation of cells by inflammatory factors and lipopolysaccharides activates the p38 MAPK pathway, causing an inflammatory cascade [41]. Excessive phosphorylation and activation of p38 MAPK were observed in spontaneous skin-scratching mice, suggesting that MAPK was activated. However, inhibiting the activation of p38 reduced skin inflammation, which is related to the suppression of the mRNA levels of TNF, IL-6, and other pro-inflammatory factors in the skin [42].

KEGG enrichment analysis of target proteins revealed that cytokine-cytokine receptor interaction, TNF, MAPK, NF-κB, toll-like receptor, T cell receptor, and Th1 and Th2 cell differentiation signaling pathways were the main treatment pathways. Notably, most of these pathways are associated with inflammatory responses, cell differentiation, and body immune responses. Cytokines, proteins that regulate cellular interactions, bind to corresponding cellular receptors to activate cell signaling and participate in cell growth, maturation, and differentiation. They are also important regulators in innate and adaptive immunity. Th2 cytokines in particular, such as IL-4, play a major role in the pathogenesis of eczema [43]. IL-4 and other Th2 cytokines can downregulate the expression of filaggrin, loricrin, and involucrin in the skin, causing skin barrier defects [44]. A clinical study has demonstrated the efficacy of dupilumab, an antagonist of IL4R, in patients with eczema [45]. Moreover, the overproduction of Th2-type cytokines leads to the activation of B cells and extensive secretion of IgE [6]. Mast cells and eosinophils sensitized by IgE can synthesize and secrete a large number of inflammatory mediators, causing pruritus, erythema, tissue edema, and other metamorphic reactions [29,46]. The excessive secretion of Th2 cytokines inhibits the proliferation and action of Th1 cells [47]; therefore, a Th1/Th2 imbalance is a common pathological feature in patients with eczema. Regulating the levels of cytokines such as IL-4 and INF-γ (Th1 cytokine) can restore the Th1/Th2 balance, which results in good therapeutic effects in patients with eczema [48,49].

Signaling pathways are complex networks that reciprocally interfere and crosstalk. For example, the toll-like receptor, NF-κB, and MAPK signaling pathways are upstream pathways that can affect Th1 and Th2 cell differentiation [50]. Toll-like receptors are natural immune recognition receptors that belong to transmembrane receptor protein families. Following external stimulation, the body upregulates toll-like receptor expression and activates NF-κB and p38 MAPK via MyD88-dependent signaling pathways, thereby amplifying inflammation. After activation of the NF-κB pathway, the NF-κB dimer is activated into the nucleus and binds to two major enhancer sites in the IL-4 locus after activation, which induces the secretion of IL-4 and contributes to Th2 differentiation [51]. The MAPK signaling pathway participates in various cellular functions such as immune cell activation, differentiation, and proliferation through cascade reactions, and also activates the NF-κB signaling pathway [52]. The differentiation of T cells into Th1 and Th2 cells is regulated by key transcription factors T-bet and GATA-3 [53]. Via the ubiquitin-proteasome-dependent pathway, p38 MAPK controls the stability of GATA3, affecting Th2 differentiation and Th2-type cytokine production [54]. The activation of the MAPK signaling pathway plays an important role in eczema, and reducing the levels of p38MAPK can inhibit the production of downstream pro-inflammatory factors and alleviate eczema symptoms [55].

In this study, we verified the therapeutic effects of SZQG in an eczema rat model. The animal experiments demonstrated that the application of SZQG reduces the mRNA expression of the key transcription factors, RELA and MAPK14, in the NF-κB and MAPK pathways and inhibits the mRNA expression of Th1 and Th2 transcription factors, T-bet and GATA3. This is conducive to reducing the secretion of IL-4 and IgE, and correcting the imbalance of Th1/Th2 cytokines. UHPLC-MS/MS showed that quercetin, luteolin, and ursolic acid were the core compounds of SZQG. Quercetin has excellent anti-inflammatory properties, such as inhibiting NF-κB activation and pro-inflammatory cytokines release in white blood cells and histamine and leukotriene inflammatory substance release by stabilizing mast cell membranes [56]. Luteolin ameliorates Th1/Th2 imbalance and their cytokine ratio by interfering with the TLR4/NF-κB pathway [57]. Ursolic acid has a positive effect on eosinophil infiltration in allergic diseases, and can reduce levels of various interleukins and IgE [58]. These results suggest that SZQG regulate immune functions in the body, exert strong anti-inflammatory effects, and alleviate the development of eczema-like lesions.

The positive control drug used in this experiment was a kind of glucocorticoid, which is commonly used in the clinical treatment of acute eczema. During the treatment process, glucocorticoid improved the exudation symptoms better in the first 2 days of treatment, implying that this hormone therapy took effect quicker, although the overall effectiveness over a week was comparable to that of SZQG. In addition, eczema is a recurrent disease, but the effect of SZQG in reducing disease recurrence has not been verified in this study.

There are some limitations in this study. First, we chose UHPLC-MS/MS to identify the compounds of SZQG in this experiment, which has a wide detection range and good separation efficacy. However, the volatile compounds in the herbal ingredients were easily lost in the process of identification and the drug components were not detected in the blood. Second, network pharmacology and animal experiments were used to preliminarily verify and explore the main mechanism of SZQG; however, more in-depth research is

required to have a clear understanding of all the mechanisms of action. To further explore the specific mechanisms of SZQG, experimental molecular techniques such as western blotting and immunohistochemistry should be utilized in future studies, placing greater emphasis on *in vitro* studies.

5. Conclusions

In this study, the mechanism of action and molecular targets of SZQG for eczema were researched using network pharmacology methods and a preclinical animal model. Based on our results, we concluded that the therapeutic effect of SZQG on eczema may involve multiple targets, pathways, and mechanisms. Among them, the core compounds, such as quercetin, luteolin, and ursolic acid, may regulate the levels of inflammatory factors by acting on NF-κB and p38 MAPK, thereby regulating the differentiation of Th1 and Th2, which ultimately alleviates of inflammation for the treatment of eczema. As a novel formulation of traditional Chinese medicine, the SZQG offer the advantage of convenient administration, overcoming the complex processing procedures associated with traditional herbal decoctions. Moreover, SZQG demonstrated promising therapeutic effects on the symptoms of eczema, making them a viable alternative treatment option for eczema patients. Our findings provide a theoretical basis for the clinical application and further exploration of the mechanisms of action of SZQG.

Funding

This research was supported by the Fundamental Research Funds for Central Universities (2020-JYB-ZDGG-016) and the National Natural Science Foundation of China (8227152963).

Data availability statement

All the original data are included in the supplementary materials.

Ethics declarations

This study was reviewed and approved by the Medical and Experimental Animal Ethics Committee of Beijing University of Chinese Medicine, with the approval number: BUCM-4-2021110806-4069.

CRediT authorship contribution statement

Hairong Zhang: Writing – review & editing, Writing – original draft. **Zhenbo Li:** Conceptualization. **Yike Sun:** Validation, Formal analysis. **Wenna Li:** Software, Resources. **Xiao Sun:** Visualization. **Yapeng Zhang:** Data curation. **Leilei Liu:** Writing – review & editing. **Shuran Ma:** Supervision, Funding acquisition.

Declaration of competing interest

The authors declare that they have no known competing financial interests or personal relationships that could have appeared to influence the work reported in this paper.

Acknowledgements

We are grateful to Dr. Shenglou Ni (Beijing University of Chinese Medicine) for his critical comments on this paper.

Appendix A. Supplementary data

Supplementary data to this article can be found online at https://doi.org/10.1016/j.heliyon.2024.e27603.

References

[1] R. Raveendran, Tips and tricks for controlling eczema, Immunol. Allergy Clin. 39 (4) (2019) 521–533.
[2] J.H. Lee, S.W. Son, S.H. Cho, A comprehensive review of the treatment of atopic eczema, Allergy Asthma Immunol. Res 8 (3) (2016) 181–190.
[3] A.T.M. Ronnstad, A.S. Halling-Overgaard, C.R. Hamann, L. Skov, A. Egeberg, J.P. Thyssen, Association of atopic dermatitis with depression, anxiety, and suicidal ideation in children and adults: a systematic review and meta-analysis, J. Am. Acad. Dermatol. 79 (3) (2018) 448–456.
[4] I.N. Belugina, N.Z. Yagovdik, O.S. Belugina, S.N. Belugin, Outdoor environment, ozone, radionuclide-associated aerosols and incidences of infantile eczema in Minsk, Belarus, J. Eur. Acad. Dermatol. Venereol. 32 (11) (2018) 1977–1985.
[5] G. Egawa, K. Kabashima, Multifactorial skin barrier deficiency and atopic dermatitis: essential topics to prevent the atopic march, J. Allergy Clin. Immunol. 138 (2) (2016) 350–358.
[6] W. David Boothe, J.A. Tarbox, M.B. Tarbox, Atopic dermatitis: pathophysiology, Adv. Exp. Med. Biol. 1027 (2017) 21–37.

[7] A. Wollenberg, S. Barbarot, T. Bieber, S. Christen-Zaech, M. Deleuran, A. Fink-Wagner, U. Gieler, G. Girolomoni, S. Lau, A. Muraro, M. Czarnecka-Operacz, T. Schafer, P. Schmid-Grendelmeier, D. Simon, Z. Szalai, J.C. Szepietowski, A. Taieb, A. Torrelo, T. Werfel, J. Ring, t.E.A.o.D. European Dermatology Forum, t.E.A.o.A. Venereology, t.E.T.F.o.AD.E.F.o.A. Clinical Immunology, t.E.S.f.D. Airways Diseases Patients' Associations t.E.S.o.P.D.G.A, Psychiatry, N, Asthma European, S, The European Union of Medical, Consensus-based European guidelines for treatment of atopic eczema (atopic dermatitis) in adults and children: part II, J. Eur. Acad. Dermatol. Venereol. 32 (6) (2018) 850–878.

[8] Z. Wang, Z.Z. Wang, J. Geliebter, R. Tiwari, X.M. Li, Traditional Chinese medicine for food allergy and eczema, Ann. Allergy Asthma Immunol. 126 (6) (2021) 639–654.

[9] J. Lu, D. Zhang, F. Cao, L. Zhang, S. Ma, X. Liu, Research on the effects of Jiuwan decoction on chronic eczema model rats, Chinese Medicine modern distance education of China 18 (14) (2020) 114–117.

[10] R. Singh, R. Purohit, Computational analysis of protein-ligand interaction by targeting a cell cycle restrainer, Comput. Methods Programs Biomed. 231 (2023) 107367.

[11] S. Kumar, V. Kumar Bhardwaj, R. Singh, R. Purohit, Explicit-solvent molecular dynamics simulations revealed conformational regain and aggregation inhibition of I113T SOD1 by Himalayan bioactive molecules, J. Mol. Liq. 339 (2021) 116798.

[12] J. Ru, P. Li, J. Wang, W. Zhou, B. Li, C. Huang, P. Li, Z. Guo, W. Tao, Y. Yang, X. Xu, Y. Li, Y. Wang, L. Yang, TCMSP: a database of systems pharmacology for drug discovery from herbal medicines, J. Cheminform. 6 (2014) 13.

[13] M.M. Zhang, D. Wang, F. Lu, R. Zhao, X. Ye, L. He, L. Ai, C.J. Wu, Identification of the active substances and mechanisms of ginger for the treatment of colon cancer based on network pharmacology and molecular docking, BioData Min. 14 (1) (2021) 1.

[14] D. Gfeller, A. Grosdidier, M. Wirth, A. Daina, O. Michielin, V. Zoete, SwissTargetPrediction: a web server for target prediction of bioactive small molecules, Nucleic Acids Res. 42 (W1) (2014) W32–W38.

[15] The Uniprot Consortium, UniProt: the universal protein knowledgebase in 2021, Nucleic Acids Res. 49 (D1) (2021) D480–D489.

[16] G. Stelzer, N. Rosen, I. Plaschkes, S. Zimmerman, M. Twik, S. Fishilevich, T.I. Stein, R. Nudel, I. Lieder, Y. Mazor, S. Kaplan, D. Dahary, D. Warshawsky, Y. Guan-Golan, A. Kohn, N. Rappaport, M. Safran, D. Lancet, The GeneCards suite: from gene data mining to disease genome sequence analyses, Curr. Protoc. Bioinformatics 54 (2016), 1.30.31-31.30.33.

[17] Y. Wang, S. Zhang, F. Li, Y. Zhou, Y. Zhang, Z. Wang, R. Zhang, J. Zhu, Y. Ren, Y. Tan, C. Qin, Y. Li, X. Li, Y. Chen, F. Zhu, Therapeutic target database 2020: enriched resource for facilitating research and early development of targeted therapeutics, Nucleic Acids Res. 48 (D1) (2020) D1031–D1041.

[18] J. Piñero, J.M. Ramírez-Anguita, J. Saüch-Pitarch, F. Ronzano, E. Centeno, F. Sanz, L.I. Furlong, The DisGeNET knowledge platform for disease genomics: 2019 update, Nucleic Acids Res. 48 (D1) (2019) D845–D855.

[19] J.S. Amberger, C.A. Bocchini, F. Schiettecatte, A.F. Scott, A. Hamosh, OMIM.org: online Mendelian Inheritance in Man (OMIM®), an online catalog of human genes and genetic disorders, Nucleic Acids Res. 43 (D1) (2015) D789–798.

[20] D.S. Wishart, Y.D. Feunang, A.C. Guo, E.J. Lo, A. Marcu, J.R. Grant, T. Sajed, D. Johnson, C. Li, Z. Sayeeda, N. Assempour, I. Iynkkaran, Y. Liu, A. Maciejewski, N. Gale, A. Wilson, L. Chin, R. Cummings, D. Le, A. Pon, C. Knox, M. Wilson, DrugBank 5.0: a major update to the DrugBank database for 2018, Nucleic Acids Res. 46 (D1) (2018) D1074–D1082.

[21] D. Szklarczyk, A.L. Gable, D. Lyon, A. Junge, S. Wyder, J. Huerta-Cepas, M. Simonovic, N.T. Doncheva, J.H. Morris, P. Bork, L.J. Jensen, C.V. Mering, STRING v11: protein-protein association networks with increased coverage, supporting functional discovery in genome-wide experimental datasets, Nucleic Acids Res. 47 (D1) (2019) D607–D613.

[22] J. Lu, X. Liu, Y. Xiao, S. Ma, Shizhenqing granule stimulates the hypothalamic-pituitary-adrenal axis and reduces serum pro-inflammatory factors in a rat model with chronic eczema, J. Tradit. Chin. Med. Sci. 7 (4) (2020) 386–392.

[23] B. Ham, M. Kim, Y.-J. Son, S. Chang, S.H. Jung, C.W. Nho, M.J. Kwon, Inhibitory effects of pterocarpus santalinus extract against IgE/antigen-sensitized mast cells and atopic dermatitis-like skin lesions, Planta Med. 85 (7) (2019) 599–607.

[24] R. Chopra, P.P. Vakharia, R. Sacotte, N. Patel, S. Immaneni, T. White, R. Kantor, D.Y. Hsu, J.I. Silverberg, Severity strata for eczema area and severity Index (EASI), modified EASI, scoring atopic dermatitis (SCORAD), objective SCORAD, atopic dermatitis severity Index and body surface area in adolescents and adults with atopic dermatitis, Br. J. Dermatol. 177 (5) (2017) 1316–1321.

[25] T.-Y. Kim, Y.J. Kim, J. Jegal, B.-G. Jo, H.-S. Choi, M.H. Yang, Haplopine ameliorates 2,4-dinitrochlorobenzene-induced atopic dermatitis-like skin lesions in mice and TNF-α/IFN-γ-induced inflammation in human keratinocyte, Antioxidants 10 (5) (2021) 806.

[26] N. Stefanovic, C. Flohr, A.D. Irvine, The exposome in atopic dermatitis, Allergy 75 (1) (2020) 63–74.

[27] C. Hulpusch, A.B. Weins, C. Traidl-Hoffmann, M. Reiger, A new era of atopic eczema research: advances and highlights, Allergy 76 (11) (2021) 3408–3421.

[28] D.-D. Zhao, X.-Q. Zhang, T. Yang, Q. Liu, Z.-Z. Lan, X.-L. Yang, H.-Y. Qu, H. Zhou, T. Hussain, Exploring the therapeutic mechanism of Tingli Dazao Xiefei decoction on heart failure based on network pharmacology and experimental study, Evid. Based Complement. Alternat. Med. 2021 (2021) 1–15.

[29] K.-I. Yamanaka, H. Mizutani, The role of cytokines/chemokines in the pathogenesis of atopic dermatitis, Curr. Probl. Dermatol. 41 (2011) 80–92.

[30] S. Tasneem, B. Liu, B. Li, M.I. Choudhary, W. Wang, Molecular pharmacology of inflammation: medicinal plants as anti-inflammatory agents, Pharmacol. Res. 139 (2019) 126–140.

[31] X. Li, Z. Tang, L. Wen, C. Jiang, Q. Feng, Matrine, A review of its pharmacology, pharmacokinetics, toxicity, clinical application and preparation researches, J. Ethnopharmacol. 269 (2020) 113682.

[32] V. Karuppagounder, S. Arumugam, R.A. Thandavarayan, V. Pitchaimani, R. Sreedhar, R. Afrin, M. Harima, H. Suzuki, M. Nomoto, S. Miyashita, K. Suzuki, M. Nakamura, K. Watanabe, Modulation of HMGB1 translocation and RAGE/NFκB cascade by quercetin treatment mitigates atopic dermatitis in NC/Nga transgenic mice, Exp. Dermatol. 24 (6) (2015) 418–423.

[33] H. Kocic, G. Damiani, B. Stamenkovic, M. Tirant, A. Jovic, D. Tiodorovic, K. Peris, Dietary compounds as potential modulators of microRNA expression in psoriasis, Ther. Adv. Chronic. Dis. 10 (2019) 2040622319864805.

[34] M. Jafarinia, M. Sadat Hosseini, N. Kasiri, N. Fazel, F. Fathi, M. Ganjalikhani Hakemi, N. Eskandari, Quercetin with the potential effect on allergic diseases, Allergy Asthma Clin. Immunol. 16 (2020) 36.

[35] S.-E. Jang, J.-J. Jeong, S.R. Hyam, M.J. Han, D.-H. Kim, Ursolic acid isolated from the seed of Cornus officinalis ameliorates colitis in mice by inhibiting the binding of lipopolysaccharide to Toll-like receptor 4 on macrophages, J. Agric. Food Chem. 62 (40) (2014) 9711–9721.

[36] R. Samivel, R.P. Nagarajan, U. Subramanian, A.A. Khan, A. Masmali, T. Almubrad, S. Akhtar, Inhibitory effect of ursolic acid on ultraviolet B radiation-induced oxidative stress and proinflammatory response-mediated senescence in human skin dermal fibroblasts, Oxid. Med. Cell. Longev. 2020 (2020) 1246510.

[37] N. Xia, G. Chen, M. Liu, X. Ye, Y. Pan, J. Ge, Y. Mao, H. Wang, J. Wang, S. Xie, Anti-inflammatory effects of luteolin on experimental autoimmune thyroiditis in mice, Exp. Ther. Med. 12 (6) (2016) 4049–4054.

[38] F. Gendrisch, P.R. Esser, C.M. Schempp, U. Wolfle, Luteolin as a modulator of skin aging and inflammation, Biofactors 47 (2) (2021) 170–180.

[39] T.-Y. Kim, Y.J. Kim, J. Jegal, B.-G. Jo, H.-S. Choi, M.H. Yang, Kaempferol modulates pro-inflammatory NF-kappaB activation by suppressing advanced glycation endproducts-induced NADPH oxidase, Age 32 (2) (2010) 197–208.

[40] Z. Wang, F. Zhuo, P. Chu, X. Yang, G. Zhao, Germacrone alleviates collagen-induced arthritis via regulating Th1/Th2 balance and NF-κB activation, Biochem. Biophys. Res. Commun. 518 (3) (2019) 560–564.

[41] M.B. Alam, Y.G. Kwon, S.Y. Simu, S. Abrar Shahriyar, S.H. Lee, Attenuation of inflammatory symptoms by icariside B2 in carrageenan and LPS-induced inflammation models via regulation of MAPK/NF-κB signaling cascades, Biomolecules 10 (7) (2020).

[42] B. Theivanthiran, M. Kathania, M. Zeng, E. Anguiano, V. Basrur, T. Vandergriff, V. Pascual, W.-Z. Wei, R. Massoumi, K. Venuprasad, The E3 ubiquitin ligase itch inhibits p38α signaling and skin inflammation through the ubiquitylation of Tab1, Sci. Signal. 8 (365) (2015) ra22.

[43] S. Park, J.B. Lee, S. Kang, Topical application of chrysanthemum indicum L. attenuates the development of atopic dermatitis-like skin lesions by suppressing serum IgE levels, IFN-γ, and IL-4 in Nc/Nga mice, Evid. Based Complement. Alternat. Med. (2012) 821967, 2012.

[44] P.M. Brunner, E. Guttman-Yassky, D.Y. Leung, The immunology of atopic dermatitis and its reversibility with broad-spectrum and targeted therapies, J. Allergy Clin. Immunol. 139 (4S) (2017) S65–S76.

[45] D. Thaçi, E.L. Simpson, L.A. Beck, T. Bieber, A. Blauvelt, K. Papp, W. Soong, M. Worm, J.C. Szepietowski, H. Sofen, M. Kawashima, R. Wu, S.P. Weinstein, N.M. H. Graham, G. Pirozzi, A. Teper, E.R. Sutherland, V. Mastey, N. Stahl, G.D. Yancopoulos, M. Ardeleanu, Efficacy and safety of dupilumab in adults with moderate-to-severe atopic dermatitis inadequately controlled by topical treatments: a randomised, placebo-controlled, dose-ranging phase 2b trial, Lancet (London, England) 387 (10013) (2016) 40–52.
[46] M. Manohar, K.C. Nadeau, The potential of anti-IgE in food allergy therapy, Curr. Treat. Options Allergy 1 (2) (2014) 145–156.
[47] Y. Yang, Y. Zhou, Shashen-Maidong decoction-mediated IFN-gamma and IL-4 on the regulation of Th1/Th2 imbalance in RP rats, BioMed Res. Int. 2019 (2019) 6012473.
[48] X. Wang, S. Li, J. Liu, D. Kong, X. Han, P. Lei, M. Xu, H. Guan, D. Hou, Ameliorative effects of sea buckthorn oil on DNCB induced atopic dermatitis model mice via regulation the balance of Th1/Th2, BMC Complement. Med. Ther. 20 (1) (2020) 263.
[49] F.-T. Liu, H. Goodarzi, H.-Y. Chen, IgE, mast cells, and eosinophils in atopic dermatitis, Clin. Rev. Allergy Immunol. 41 (3) (2011) 298–310.
[50] K. Maeda, M.J. Caldez, S. Akira, Innate immunity in allergy, Allergy 74 (9) (2019) 1660–1674.
[51] H. Oh, S. Ghosh, NF-kappaB: roles and regulation in different CD4(+) T-cell subsets, Immunol. Rev. 252 (1) (2013) 41–51.
[52] H.J. Fan, X.S. Zhao, Z.B. Tan, B. Liu, H.L. Xu, Y.T. Wu, L.P. Xie, Y.M. Bi, Y.G. Lai, H.F. Liang, Y.C. Zhou, Effects and mechanism of action of Huang-Lian-Jie-Du-Tang in atopic dermatitis-like skin dysfunction *in vivo* and *in vitro*, J. Ethnopharmacol. 240 (2019) 111937.
[53] A. Hertweck, M. Vila de Mucha, P.R. Barber, R. Dagil, H. Porter, A. Ramos, G.M. Lord, R.G. Jenner, The TH1 cell lineage-determining transcription factor T-bet suppresses TH2 gene expression by redistributing GATA3 away from TH2 genes, Nucleic Acids Res. 50 (8) (2022) 4557–4573.
[54] K. Maneechotesuwan, Y. Xin, K. Ito, E. Jazrawi, K.Y. Lee, O.S. Usmani, P.J. Barnes, I.M. Adcock, Regulation of Th2 cytokine genes by p38 MAPK-mediated phosphorylation of GATA-3, J. Immunol. 178 (4) (2007) 2491–2498.
[55] B. Sur, S. Kang, M. Kim, S. Oh, Alleviation of atopic dermatitis lesions by a benzylideneacetophenone derivative via the MAPK signaling pathway, Inflammation 42 (3) (2019) 1093–1102.
[56] J. Mlcek, T. Jurikova, S. Skrovankova, J. Sochor, Quercetin and its anti-allergic immune response, Molecules 21 (5) (2016) 623.
[57] J. Dong, O. Xu, J. Wang, C. Shan, X. Ren, Luteolin ameliorates inflammation and Th1/Th2 imbalance via regulating the TLR4/NF-κB pathway in allergic rhinitis rats, Immunopharmacol. Immunotoxicol. 43 (3) (2021) 319–327.
[58] N. Sun, Z. Han, H. Wang, Z. Guo, C. Deng, W. Dong, G. Zhuang, R. Zhang, Effects of ursolic acid on the expression of Th1-Th2-related cytokines in a rat model of allergic rhinitis after PM2.5 exposure, Am. J. Rhinol. Allergy 34 (5) (2020) 587–596.